Edge Currents in Superconductors with a Broken Time-Reversal Symmetry

Bernd Braunecker,[1,2] Patrick A. Lee,[1] and Ziqiang Wang[3]
[1]*Department of Physics, Massachusetts Institute of Technology, Cambridge, Massachusetts 02139, USA*
[2]*Department of Physics, Brown University, Providence, Rhode Island 02912, USA*
[3]*Department of Physics, Boston College, Chestnut Hill, Massachusetts 02467, USA*
(Received 7 January 2005; published 1 July 2005)

We analyze edge currents and edge bands at the surface of a time-reversal symmetry breaking $d_{x^2-y^2} + id_{xy}$ superconductor. We show that the currents have large Friedel oscillations with two interfering frequencies: $\sqrt{2}k_F$ from subgap states, and $2k_F$ from the continuum. The results are based independently on a self-consistent slave-boson mean-field theory for the t-J model on a triangular lattice, and on a T-matrix scattering theory calculation. The shape of the edge-state band, as well as the particular frequency $\sqrt{2}k_F$ of the Friedel oscillations, are attributes unique for the $d_{x^2-y^2} + id_{xy}$ case, and may be used as a fingerprint for its identification. Extensions to different time-reversal symmetry breaking superconductors can be achieved within the same approach.

DOI: 10.1103/PhysRevLett.95.017004 PACS numbers: 74.25.Jb, 71.27.+a, 74.20.Rp

Superconductors that break time-reversal symmetry have attracted a great deal of attention recently. The most prominent example is Sr_2RuO_4, which has a p-type complex order parameter [1]. There have been theoretical suggestions that $Na_xCoO_2 \cdot yH_20$ belongs to this class, but with complex d-wave symmetry [2–4]. It is known that interesting edge effects are induced by the surface in such superconductors. First, the surface induces the appearance of an edge band inside the superconducting gap. Second, a chiral edge current parallel to the surface appears. As shown in several independent semiclassical calculations [5–8], the shape of the dispersion ϵ_b of the edge states depends on the symmetry of the superconductor and may be used as a fingerprint for the latter. In this Letter, we quantitatively address this problem and point out a novel interference in the edge current which distinguishes between $d_{x^2-y^2} + id_{xy}(\equiv d + id')$ and complex p time-reversal symmetry breaking superconductors. We perform a self-consistent solution of the t-J model on a triangular lattice which has a $d + id'$ superconducting phase as the solution of its slave-boson mean-field theory [2–4]. In order to explain the novel results uncovered by the numerical solution, we analytically solve a quantum continuum model by treating the quasiparticle scattering on the surface using an extension of the T-matrix formulation of [9].

The results are summarized as follows (see Fig. 1): The surface induces edge currents and an edge band in agreement with the semiclassical prediction of two parts of a parabola [8], $\epsilon_b(k_x) = -\Delta \mathrm{sgn}(k_x)(2k_x^2/k_F^2 - 1)$. As a surprising novel result, the size and direction of the current changes rapidly with distance from the surface. This is interpreted as Friedel oscillations of *two* frequencies, $2k_F$ and $\sqrt{2}k_F$. The $2k_F$ oscillations are the usual Friedel oscillations of the continuum states. The $\sqrt{2}k_F$ oscillations are due to the zero energy mode of the subgap band, $\epsilon_b = 0$, and correspond to a quasiparticle scattering on the surface at an incident angle of 45° [6] [Fig. 1(a) inset]. Most notably, the amplitudes of both oscillations are identical, and comparable to the nonoscillating part of the current; from the self-consistent numerical results we see that they are, indeed, large enough to reverse the current direction in some regions close to the surface. The overall magnitude of the edge current, therefore, is considerably smaller than could be expected naively. Our calculations lead to an integral edge current I of the order of 60 nA, which also corresponds roughly to its maximal amplitude. Such a current may be captured by measuring the induced magnetic field B. For our model calculations, we estimate its maximum at the surface as $B = \mu_0 I/2\pi\xi \sim 0.1$ G, where ξ is the coherence length of the superconductor.

The t-J model on a two-dimensional triangular lattice is an example of a microscopic model with a $d + id'$ superconducting phase as the result of the slave-boson mean-field theory [2–4]. We solve the mean-field theory self-consistently in real space following the approach by [10] in the presence of two surfaces on the top and bottom of the system. The model Hamiltonian is the t-J model plus a long-range Coulomb repulsion,

$$H = -t\sum_{\langle ij\rangle}(c_{i\sigma}^\dagger c_{j\sigma} + \mathrm{H.c.}) + J\sum_{\langle ij\rangle}\left(\mathbf{S}_i \cdot \mathbf{S}_j - \frac{n_i n_j}{4}\right) + \sum_i V_i n_i, \quad (1)$$

where $\langle ij\rangle$ runs over the nearest neighbors lattice sites of an equilateral triangular lattice, $c_{i\sigma}$ are the electron operators, and $\mathbf{S}_i$ the spin 1/2 operator. The model is completed by the constraint $n_i = \sum_\sigma c_{i\sigma}^\dagger c_{i\sigma} \leq 1$. $J > 0$ is the antiferromagnetic exchange interaction, and t the hopping integral. Because of the missing particle-hole symmetry on the triangular lattice, the sign of t is important [2,3]. We choose $t/J = -3$, corresponding to electron doping of the system. $V_i = V_c \sum_{j\neq i}(n_j - \bar{n})/|\mathbf{r}_i - \mathbf{r}_j|$ is the Coulomb potential felt by the particle at the site i, where $\bar{n}$ is the average density, j runs over all lattice sites, and $V_c \approx 5J$ [10]. The long-range Coulomb interaction is necessary to overrule the inherent tendency of the mean-field theory to phase separate. In a uniform system, V_i vanishes. On the lightly doped triangular lattice, however, the Coulomb interaction alone is not strong enough against the phase separating instabilities. The key insight for a stabilization is the correction of the mean-field theory by a Jastrow-like modification of the hopping parameter $t \rightarrow t\exp(-w|\sqrt{(1-n_i)(1-n_j)} - (1-\bar{n})|)$ for nearest neighbor sites with $w \sim 5$. This factor suppresses the gain in kinetic energy by clustering carriers on neighboring sites. For small fluctuations in the carrier concentrations, it is close to 1. Its precise form otherwise has not much influence.

In the slave-boson formulation, the electron operator is decomposed as $c_{i\sigma} = f_{i\sigma} b_i^\dagger$, where $f_{i\sigma}$ is a spin carrying fermion, and b_i a charge carrying boson operator. The constraint $n_i \leq 1$ becomes the identity $\Sigma_\sigma f_{i\sigma}^\dagger f_{i\sigma} + b_i^\dagger b_i = 1$, which must be fulfilled at each site i, and which can be included in the action with Lagrange multipliers λ_i.

In the superconducting phase, the bosons b_i are condensed and directly related to the local carrier concentrations, $x_i = (1 - n_i) = b_i^2$. The (Jastrow-corrected) mean-field theory can be derived by a variational ansatz [11], and leads to a Hamiltonian for the fermion fields $f_{i\sigma}$, expressed in terms of the x_i, the hopping parameter $\chi_{ij} = \langle f_{i\sigma}^\dagger f_{j\sigma} \rangle$, and the pairing parameter $\Delta_{ij} = \langle f_{i\uparrow} f_{j\downarrow} - f_{i\downarrow} f_{j\uparrow} \rangle$. The theory is solved self-consistently by iteration: For random initial order parameters, we solve the Bogoliubov–de Gennes equations by diagonalization of the Hamiltonian. The resulting spectrum and wave functions are used to reconstruct the order parameters and the local densities. The Lagrange multipliers λ_i are calculated explicitly by minimizing the action with respect to the condensed bosons b_i. This is repeated until convergence and requires up to 1000 iterations.

We study lattices consisting in a strip with periodic boundary conditions along the x direction and, to model the two surfaces, open boundary conditions along the y direction. To reduce the interference between the edges, we choose systems in which the surfaces are far apart (typically $\sim$100 lattice sites). Finite size constraints are important and distort the perfect $d + id'$ symmetry in that the phase difference of Δ_{ij} between lattice directions deviates from $2\pi/3$, or that the ratio $\mathrm{Re}\Delta_{ij}/\mathrm{Im}\Delta_{ij}$ in the bulk deviates from unity. To minimize these effects, we choose a sufficiently large extension along the x direction of $N_x = 24$. In Fig. 1(a) (circles) we show the resulting edge current. It has oscillations with a large amplitude that lead at some layers to the reversal of the current direction. The spatial period of the oscillations is roughly twice the lattice spacing, but beatings indicate a frequency mixture. The multiplication of the displayed current by $te/\hbar$ (e = electron charge) provides the current in amperes. With $t = -3J$ and $J = 20$ meV (as estimated for the Na_xCoO_2 superconductor as a candidate for the $d + id'$ symmetry [2–4]), the overall current, integrated along the direction perpendicular to the surface, is about 60 nA (setting an order of magnitude), and is concentrated within a few times the decay length of $\xi_{\mathrm{cur}} \approx 5a$ (with $a \approx 3$ Å the lattice constant for the equilateral triangular lattice).

Figure 1(b) shows the spectrum of the system as a function of k_x after a Fourier transformation of the real-space result. We have suppressed the edge states at one of the two surfaces by inspection of the support of the wave functions. An asymmetric subgap band is clearly visible. Its shape deviates slightly from the parabola predicted from the semiclassical arguments as an effect of the discrete and finite lattice and the variation of the magnitude of Δ close to the edge. In particular, a small gap persists due to the limited system size and the interference between the edges. The gap closes with increasing distance of the surfaces.

A similar computation can be performed for a lattice with a single site defect [12]. Instead of a band, a pair of bound states appears at the defect site. For similar interaction parameters, the edge current is concentrated on the immediate neighbors of the defect site only, and has a value of about 100 nA. This leads to a magnetic field of the order of 1 G on the defect site.

The large amplitude of the oscillations seems to be surprising, but can be derived within a continuum model for the scattering on the surface. The calculation must go

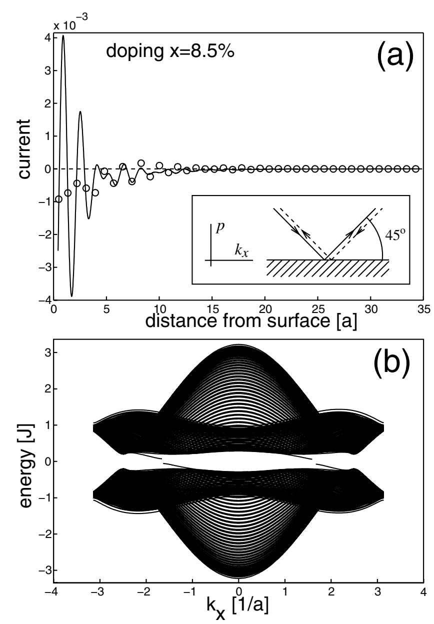

FIG. 1. (a) Current (in dimensionless units) from the self-consistent calculation (circles) and the prediction of Eqs. (10) and (12) multiplied by an exponential decay factor $\exp(-y/\xi_{\mathrm{cur}})$ (full line). The inset shows the quasiclassical Andreev scattering on the surface leading to the $\sqrt{2}k_F$ oscillations (full lines: particle scattering; dashed lines: hole scattering). (b) Spectrum E_{n,k_x} as a function of the momentum k_x; n is the quantization along the y direction. Continuum states form the hatlike structures, the subgap states have roughly parabolic forms. The small gap at zero energy is a finite size effect due to the coupling between the two edges.

beyond the semiclassical arguments, and we follow the T-matrix calculation by [9], which we extend for the calculation of the current density $j(y)$. Even though we focus on the $d + id'$ symmetry, the approach is general and can be extended to any given symmetry of the superconductor. We consider a semi-infinite two-dimensional $d + id'$ superconductor in the (x, y) plane with its surface at $y = 0$, and the superconductor at $y > 0$. The current can be obtained from the causal (time-ordered) Green's function, $G^c(\mathbf{x}, \mathbf{x}'; t)$, by the expression

$$j(\mathbf{x}) = \frac{1}{2m} \sum_{\sigma=\uparrow,\downarrow} (\nabla_{\mathbf{x}} - \nabla_{\mathbf{x}'}) G^c_\sigma(\mathbf{x}, \mathbf{x}'; t = 0^-)|_{\mathbf{x}'=\mathbf{x}}, \quad (2)$$

with m the mass of the carriers. In contrast to [9], causal instead of retarded Green's functions must be used. For the $d + id'$ superconductor, we write the gap function in the simplified, position independent form $\Delta_{\mathbf{k}} = \Delta e^{2i\theta}$, where θ is the angle of the momentum $\mathbf{k}$ to a given axis. Since we intend here to provide an explanation to the observed oscillations while keeping the calculation as simple as possible, we assume $|\Delta|$ to be constant even in the vicinity of the surface. The variability of Δ is taken into account, however, in the self-consistent numerical solution above. Since the amplitude of the gap is independent of the direction, the orientation of the surface is of no importance. In this approximation, the Fermi surface is assumed to be cylindrical. The surface is modeled by a line of scattering centers with elastic potentials V, which eventually we let tend to infinity. The preserved translation symmetry along the x axis allows us to keep the momenta parallel to the surface, k_x, so that the scattering equation reads, for a given frequency ω

$$\mathbf{G}^c_{k_x}(y, y') = \mathbf{g}^c_{k_x}(y - y') + \mathbf{g}^c_{k_x}(y)\mathbf{T}_{k_x}\mathbf{g}^c_{k_x}(-y'), \quad (3)$$

where the bold symbols denote functions in the particle-hole Nambu space. The free causal Green's function, $\mathbf{g}^c_{k_x}(y)$, is

$$\mathbf{g}^c_{k_x}(y;\omega) = -\frac{\pi N_0}{p\sqrt{\Delta^2 - \omega^2} - i0} e^{-(yk_F/4p\xi)\sqrt{1-(\omega/\Delta)^2}} \times \{\omega\cos(py)\boldsymbol{\tau}_0 + \Delta \sum_{\nu=\pm} \cos(py + \nu 2\theta)\boldsymbol{\tau}_\nu\}, \quad (4)$$

where N_0 is the density of states at the Fermi energy, k_F the Fermi vector, $p = \sqrt{k_F^2 - k_x^2}$, and ξ the coherence length. Here $k_x = k_F\cos(\theta)$, $p = k_F\sin(\theta)$, $\theta \in [0, \pi]$. The $\boldsymbol{\tau}_\pm = \boldsymbol{\tau}_x \pm i\boldsymbol{\tau}_y$ are the Pauli matrices in the Nambu space; $\boldsymbol{\tau}_0$ is the unit matrix.

The T matrix is defined by $\mathbf{T}^{-1}_{k_x}(\omega) = V\boldsymbol{\tau}_z - \mathbf{g}^c_{k_x}(\omega)$. To model the surface, we let $V \to \infty$. With $\Omega = \sqrt{\Delta^2 - \omega^2} - i0$ and Eq. (4) this leads to

$$\mathbf{T} = \frac{p\Omega/\pi N_0}{\omega^2 - \Delta^2\cos^2(2\theta)(1 - i0)} \begin{pmatrix} \omega & -\Delta\cos(2\theta) \\ -\Delta\cos(2\theta) & \omega \end{pmatrix}. \quad (5)$$

In this expression we still have scattering between physical $y > 0$ states and unphysical $y < 0$ states. It contains two subgap bands with the energies $\epsilon_b^{(1,2)}(k_x) = \pm\Delta\cos(2\theta)$ for the states defined for $y > 0$ and $y < 0$, respectively. The T matrix must be split into two parts acting on those states separately. For the time-reversal symmetry breaking superconductor, we expect an asymmetry of these bands with respect to the sign of k_x, leading to the only possible choice

$$\epsilon_b^{(1)}(k_x) = -\mathrm{sgn}(k_x)\Delta\cos(2\theta) = -\mathrm{sgn}(k_x)\Delta\left(2\frac{k_x^2}{k_F^2} - 1\right), \quad (6)$$

and $\epsilon_b^{(2)} = -\epsilon_b^{(1)}$. This is precisely the expression obtained from the semiclassical models [5,8], and we can focus on the subgap band $\epsilon_b^{(1)}(k_x) \equiv \epsilon_b(k_x)$ only, relevant for $y > 0$. The splitting is achieved by writing $1/[(\omega - \epsilon_b^{(1)}) \times (\omega - \epsilon_b^{(2)})]$ as the sum and difference of $1/(\omega - \epsilon_b^{(1,2)})$, such that the remaining factors in the T matrix (5) compensate any unphysical singularity due to this decomposition. The T-matrix becomes, without the $y < 0$ part,

$$\mathbf{T}_{k_x}(\omega) = \frac{p\Omega/2\pi N_0}{\omega - \epsilon_b(k_x)(1 - i0)} \begin{pmatrix} 1 & \mathrm{sgn}(k_x) \\ \mathrm{sgn}(k_x) & 1 \end{pmatrix}. \quad (7)$$

In (k_x, y, ω) space, the current density (2) then reads (using $N_0 = m/2\pi$)

$$\begin{aligned} j(k_x, y; \omega) &= \frac{2ik_x}{m}[\mathbf{g}^c_{k_x}(y;\omega)\mathbf{T}_{k_x}(\omega)\mathbf{g}^c_{k_x}(-y;\omega]_{11} \\ &= \frac{ik_x}{2p\Omega} \frac{e^{-(yk_F/2p\xi)\sqrt{1-(\omega/\Delta)^2}}}{\omega - \epsilon_b(1 - i0)}\{\cos^2(py)(\omega \\ &\quad - \epsilon_b)^2 - \Delta\sin(2py)|\sin(2\theta)|(\omega - \epsilon_b) \\ &\quad + \Delta^2\sin^2(py)\sin^2(2\theta)\}. \end{aligned} \quad (8)$$

The ω integration leads to two contributions, the subgap poles, which exist for $\omega = \epsilon_b < 0$ only, and an integral running along the continuum state branch cut at $\omega < -\Delta$. For the subgap states, we obtain (see also [8])

$$j^{sg}(y) = \frac{-\Delta}{4\pi}\int_{-k_F}^{k_F} dk_x \frac{k_x}{p} e^{-(y/\xi)|\cos(\theta)|}\sin^2(py) \times |\sin(2\theta)|\Theta(-\epsilon_b), \quad (9)$$

with Θ the unit step function. Close to the surface, $y \ll \xi$, we can replace the exponential by unity. At $y \approx 0$, the current grows as y^2. For $yk_F \gg 1$ but still $y \ll \xi$, the integrand oscillates rapidly, and, to leading order in $1/k_F y$, j^{sg} can be estimated as

$$j^{sg}(y) = (\Delta k_F/4\pi)[1/3\sqrt{2} - \sin(\sqrt{2}k_F y)/2k_F y], \quad (10)$$

i.e., the spatial oscillations are determined by the zero energy mode of quasiparticle scattering on the surface, for which $p = k_F/\sqrt{2}$ [6] [see Fig. 1(a), inset]. Constant contributions at the artificial cutoffs at $k_x = \pm k_F$ have been neglected. For y exceeding the coherence length ξ, this current is suppressed exponentially. This allows us to identify $\xi_{\mathrm{cur}} = \xi$.

In a time-reversal symmetry breaking superconductor the continuum states carry a current, too. Their contribution is given from the ω integral running along the branch cut at $(-\infty, -\Delta)$. We restrict the integration over k_x to positive values, and keep only terms that are even in k_x. This yields $(\omega \to -\omega)$

$$j^c(y) = \frac{N_0}{\pi m} \int_0^{k_{\mathrm{F}}} \frac{dk_x k_x \epsilon_b}{p} \int_\Delta^\infty d\omega \frac{\cos(\frac{y k_{\mathrm{F}}}{2p\xi}\sqrt{(\frac{\omega}{\Delta})^2 - 1})}{\sqrt{\omega^2 - \Delta^2}} \times \frac{(\omega^2 - \Delta^2)\cos^2(py) + \Delta^2 \sin^2(2\theta)\cos(2py)}{(\omega^2 - \Delta^2) + \Delta^2 \sin^2(2\theta)}. \tag{11}$$

The integral weight is dominated by the singularity $1/\sqrt{\omega^2 - \Delta^2}$ and is concentrated at the physically relevant values of $\omega \approx \Delta$. In this region, the last factor in Eq. (11) varies slowly about $\cos(2py)$, and we replace it by this quantity. For $y \gg \xi$, the ω integration provides a Bessel function that accounts for the required exponential decay. At $y = 0$, however, the ω integration reduces to the integration of $1/\sqrt{\omega^2 - \Delta^2}$, which is divergent. This is an artifact of the approximation of a constant N_0. The integral must be cut off at the band edge where the density of states vanishes and, therefore, is given solely by its value at $\omega = \Delta$, $\int d\omega/\sqrt{\omega^2 - \Delta^2}|_\Delta = \pi/2$. For y close to the surface, we replace the ω integral by this value. The remaining k_x integration is elementary. We obtain for $y \ll \xi$, to leading order in $1/k_{\mathrm{F}} y$,

$$j^c(y) = (\Delta k_{\mathrm{F}}/4\pi)\sin(2k_{\mathrm{F}} y)/2k_{\mathrm{F}} y. \tag{12}$$

The full current density, $j(y)$, is the sum of Eqs. (10) and (12), and shows Friedel-like spatial oscillations with the two frequencies $\sqrt{2}k_{\mathrm{F}}$ and $2k_{\mathrm{F}}$.

Even though details vary in real physical systems and, as shown above, in fully self-consistent solutions, these expressions make the following precise statements: (i) The edge-state dispersion is identical to the semiclassical results [5,8]. (ii) There are two interfering Friedel oscillations of the same amplitude with the frequencies $\sqrt{2}k_{\mathrm{F}}$ and $2k_{\mathrm{F}}$, where the former is determined by the condition $\epsilon_b(k_x) = 0$. (iii) Most notably, the amplitude of the oscillations is comparable to the nonoscillating term in the current; i.e., it can reverse the direction of the current in some regions close to the surface. The exact ratio of the amplitudes cannot be captured with the present (not self-consistent) calculation. Yet the self-consistent numerical calculation above shows that this is, indeed, the case (Fig. 1). (iv) The current amplitude is proportional to Δ and k_{F}.

Friedel oscillations with the same two frequencies are found for the carrier density, $n(y)$, since it connects to the Green's function through $n(y) = -2i[\mathbf{G}^c(y, y; t = 0^-)]_{11}$.

We also note that in the spin-zero subgap band of a $p_x + ip_y$ superconductor with $\Delta_k = \Delta e^{i\theta}$ [9] the same calculation leads to $\epsilon_b \sim k_x$, which vanishes at $p = k_{\mathrm{F}}$. This provides a frequency $2k_{\mathrm{F}}$ for the Friedel oscillations from the subgap contribution and is indistinguishable from the continuum state oscillations.

From the spectrum in Fig. 1(b), we obtain $k_x \approx 2.2/a$ at $\epsilon_b = \Delta$, and $k_x \approx 1.6/a$ at $\epsilon_b = 0$, with a ratio of precisely $\sqrt{2}$. With these two values, and Δ taken from the bulk of the lattice, we can superpose the numerical result with the theoretical expressions (10) and (12). We complete the theoretical expression by a decay factor $e^{-y/\xi_{\mathrm{cur}}}$. Keeping Δ and k_{F} fixed, we fit the data for ξ_{cur}, the effective distance between the surface and the first lattice layer, and the value of the nonoscillating part (replacing the $1/3\sqrt{2}$). The resulting curve shows a nice agreement between the theoretical and numerical currents [Fig. 1(a)]. We deduce a $\xi_{\mathrm{cur}} \approx 5a$, and a nonoscillating part, which is an order of magnitude below the prediction of $1/3\sqrt{2}$. The integration of both the theoretical and numerical currents leads to an integral current of 60 nA.

To conclude, we have shown with two independent calculations that two types of Friedel oscillations exist in the time-reversal symmetry breaking superconductor, and that they play an essential role in the surface effects. The expected integral edge current and the induced magnetic field is reduced by about an order of magnitude with respect to the estimates for a nonoscillating prediction, which has important consequences for experiments.

We thank Sung-Sik Lee, J. B. Marston, and K. A. Moler for helpful discussions. B. B. acknowledges the support of the Swiss National Science Foundation, P. A. L. acknowledges the support of the DOE Grant No. DE-FG02-03ER45076, Z. W. acknowledges DOE Grant No. DE-FG02-99ER45747 and ACS Grant No. 39498-AC5M.

[1] A. P. Mackenzie and Y. Maeno, Rev. Mod. Phys. **75**, 657 (2003).
[2] G. Baskaran, Phys. Rev. Lett. **91**, 097003 (2003).
[3] Q.-H. Wang, D.-H. Lee, and P. A. Lee, Phys. Rev. B **69**, 092504 (2004).
[4] B. Kumar and B. S. Shastry, Phys. Rev. B **68**, 104508 (2003); **69**, 059901(E) (2004).
[5] C. Honerkamp and M. Sigrist, J. Low Temp. Phys. **111**, 895 (1998).
[6] T. Senthil, J. B. Marston, and M. P. A. Fisher, Phys. Rev. B **60**, 4245 (1999).
[7] M. Matsumoto and M. Sigrist, J. Phys. Soc. Jpn. **68**, 994 (1999).
[8] B. Horovitz and A. Golub, Phys. Rev. B **68**, 214503 (2003).
[9] Q.-H. Wang and Z. D. Wang, Phys. Rev. B **69**, 092502 (2004).
[10] Z. Wang *et al.*, Phys. Rev. B **65**, 064509 (2002).
[11] J. Brinckmann and P. A. Lee, Phys. Rev. B **65**, 014502 (2002).
[12] B. Braunecker, P. A. Lee, and Z. Wang (to be published).